

# Shape analysis of clusterized neutron rich matter

M. Ángeles Pérez-García

Received: 3 August 2009 / Accepted: 1 September 2009 / Published online: 25 September 2009  
© Springer Science+Business Media, LLC 2009

**Abstract** In this contribution a method for mathematically modelling clusterized nuclear matter shapes is presented. To describe shapes each cluster surface is considered as a function of spherical coordinates  $(r, \theta, \phi)$  on the unit sphere. We present an efficient approach to describe this shape function by the coefficients of a spherical harmonics expansion. Any (square-integrable) function on the unit sphere can be expanded in this manner and therefore the same methodology can be applied to enhance the description by including other observable properties such as the moment of inertia and root mean square radius of nuclear clusters.

**Keywords** Spherical harmonics · Shapes · Neutron rich matter · Neutron stars

## 1 Introduction

Compact astronomical objects such as neutron stars are believed to be composed of neutron rich matter. Their internal structure is supposed to be layered with decreasing density as stellar radius increases. In one of the outer layers, the *crust*, non-uniformities form in neutron rich matter due to the competition among long range Coulomb and short range strong interaction. This type of clusterized neutron rich matter is known generically with the name of *pasta* [1, 2]. This layer constitutes less than 10% of the mass of a typical neutron star with  $M \approx 1.5M_{\text{sun}}$  and  $R \approx 10^{-5}R_{\text{sun}}$ , however, it is crucial in the dynamics and later evolution after the early neutrino cooling stage. Neutrinos are produced in vast quantities and are responsible for the deleptonization of the star from the hot lepton rich object originating in the aftermath of a Supernova explosion.

---

M. Á. Pérez-García (✉)  
Department of Fundamental Physics and IUFFyM, University of Salamanca,  
Plaza de la Merced s/n, Salamanca 37008, Spain  
e-mail: mperezga@usal.es

It has been shown elsewhere [3] that the formation of clustered structures greatly enhance the neutrino opacities since the neutrino can coherently scatter the aggregates of nuclear matter. Then, in an analogous way to the coherent scattering of light from a periodic array, the resulting intensity can be characterized by a structure function,  $S(k)$ , where  $k = \frac{2\pi}{\lambda}$  is the typical momentum associated to the photon wavelength  $\lambda$  of the incoming light. Then the enhanced response effects due to incoming neutrinos scattering off clusters in this low density stellar region can be obtained.

The structural properties of this type of matter can be studied using many-body techniques that allow the inclusion of nuclear correlations beyond first order. Effective field theories [4] using hadronic fields either in the mean field or random phase approximation have provided satisfactory descriptions of a large set of nuclei. Other approaches, like Monte Carlo [5], classical molecular dynamics [6] in combination with adaptive integrators [7] or the antisymmetrized molecular dynamics [8] are also well suited for describing these interacting hadronic systems. In particular, finite nuclear systems such as medium mass nuclei have been described well using these approaches [9, 10]. In this type of treatments it is assumed that nucleons (protons and neutrons) are classical particles and their dynamics are governed by a given Hamiltonian depending on positions and momenta of the interacting particles at a given density,  $\rho$ , and temperature,  $T$ .

The structure of this manuscript is as follows. In Sect. 2 we briefly describe the interaction model used in our simulations of neutron rich matter. In Sect. 3 we present some simulation results and conclude.

## 2 Interaction model

We model a charge-neutral system of protons ( $Z$ ), neutrons ( $N$ ) and a background of electrons. The electrons are assumed to be a degenerate free Fermi gas of density equal to that of protons,  $\rho_e = \rho_p$ . In this semiclassical approach nucleons interact via an effective potential. Temperature should be considered as a parameter to somewhat simulate zero-point motion of the fermionic sector. The Hamiltonian describing the interaction of the nuclear system of  $A$  nucleons consists of kinetic and potential terms and reads,

$$H = \sum_{i=1}^A \frac{p_i^2}{2m} + V_{\text{tot}} , \quad (1)$$

The total potential energy,  $V_{\text{tot}}$ , is assumed to be a sum over two-body interactions  $V(i, j)$  of the following form

$$V_{\text{tot}} = \sum_{i < j=1}^A V(i, j) , \quad (2)$$

where the “elementary” two-body interaction is given by

$$V(i, j) = ae^{-r_{ij}^2/\Lambda} + [b + c\tau_z(i)\tau_z(j)]e^{-r_{ij}^2/2\Lambda} + V_c(i, j) . \quad (3)$$

Here the distance between the  $i$ th and  $j$ th particles is denoted by  $r_{ij} = |\mathbf{r}_i - \mathbf{r}_j|$  and the isospin of the  $j$ th particle is  $\tau_z(j) = 1$  for a proton and  $\tau_z(j) = -1$  for a neutron. The model parameters  $a, b, c,$  and  $\Lambda$  in the two-body interaction Eq. (3) were adjusted in Ref. [2] to reproduce the saturation density and binding energy per nucleon of symmetric nuclear matter, the binding energy per nucleon of neutron matter at saturation density, and binding energy of a few selected finite nuclei. The temperature was arbitrarily fixed at 1 MeV for all these calculations. The parameter set in the potential employed in these calculations is  $a = 110, b = -26, c = 24$  MeV and  $\Lambda = 1.25$  fm<sup>2</sup>.

This interaction, even if simplified, includes the characteristic intermediate range attraction and short-range repulsion of the nucleon–nucleon ( $NN$ ) force. Finally, a screened Coulomb interaction of the following form is included

$$V_c(i, j) = \frac{e^2}{r_{ij}} e^{-r_{ij}/\lambda} \tau_p(i) \tau_p(j) , \tag{4}$$

where  $e$  is the electron charge and  $\tau_p(j) = (1 + \tau_z(j))/2$  and  $\lambda$  is the screening length that results from the slight polarization of the electron gas. That is, the relativistic Thomas-Fermi screening length is given by  $\lambda = \frac{\pi}{e} \left( k_F \sqrt{k_F^2 + m_e^2} \right)^{-1/2}$ . Note that the electron Fermi momentum has been defined by  $k_F = (3\pi^2 \rho_e)^{1/3}$  and  $m_e$  is the electron mass.

At the low densities of interest in this work ( $10^{11} - 10^{13}$  g/cm<sup>3</sup>) we would like to explore a set of observables that we now list

– Moment of inertia

The moment of inertia can be defined generically as a tensor,  $I_{ij}$ , whose components ( $i, j = 1, \dots, 3$ ) for a body composed of  $A^c$  particles of mass  $m_k$  are,

$$I_{ij} = \sum_{k=1}^{A^c} m_k \left( \mathbf{r}_k^2 \delta_{ij} - x_{ki} x_{kj} \right) \tag{5}$$

This observable is related to the quadrupole moment that can be experimentally measured for some isotopic chains like, for example, that of carbon [11]

– Volume

The volume of the cluster can be obtained as an integration over the solid angle

$$V = \int \frac{1}{3} r^3(\theta, \phi) d\Omega \tag{6}$$

– Surface area

For a “star-like” cluster where each ray from the center of mass aims to only one point on the surface. The area can be obtained as an integral over the differential surface element

$$S = \int r \left[ r_\phi^2 + r_\theta^2 \sin^2(\theta) + r^2 \sin^2(\theta) \right]^{1/2} d\phi d\theta \tag{7}$$

where  $r_{\phi, \theta}$  are partial derivatives of  $r$  with respect to  $\phi, \theta$ .

A further measure of experimentally accessible nuclei can be obtained using an averaged spherical size using the root mean square (RMS) radius for clusters composed each of  $A^c = A_p^c + A_n^c$  nucleons. For neutrons the RMS radius,  $\langle r_n^2 \rangle^{1/2}$ , and for protons,  $\langle r_p^2 \rangle^{1/2}$ , can be expressed in the following way

$$\langle r_{p,n}^2 \rangle^{1/2} = \left[ \frac{1}{A_{p,n}^c} \sum_{i=1}^{A_{p,n}^c} \sum_{j=1}^3 (x_{ij})_{p,n}^2 \right]^{1/2} \quad (8)$$

Then, for nuclei where there is a neutron excess ( $N > Z$ ) we can define a neutron skin as the difference of the neutron and proton RMS radius

$$r_{NS} = \langle r_n^2 \rangle^{1/2} - \langle r_p^2 \rangle^{1/2} \quad (9)$$

In order to characterize the shape of the clusters we can describe the divergence from the spherical shape of the nuclear aggregates that arise from the frustrated system if we consider an orthonormal set of spherical harmonic functions [12],  $Y_{lm}(\theta, \phi)$ , with  $-l \leq m \leq l$ . The spherical angles  $\theta$  and  $\phi$  plus the radius,  $r$ , are the coordinates required to map any point on the surface of a sphere,  $S_2$ . As usual the spherical harmonics are orthogonal for different  $l$  and  $m$ , and they are normalized so that their integrated square over the sphere is unity. We use the fact that the spherical harmonics are associated to the Legendre polynomials and can write,

$$Y_{l,m}(\theta, \phi) = \sqrt{\frac{(2l+1)(l-m)!}{4\pi(l+m)!}} P_l^m(\cos \theta) e^{im\phi} \quad (10)$$

We can expand the cluster shape

$$r(\theta, \phi) = \sum_{l=0}^{\infty} \sum_{m=-l}^l a_{lm} Y_{l,m} \quad (11)$$

The expansion coefficient,  $a_{lm}$ , can be obtained by multiplying the above equation by the complex spherical harmonic,  $Y_{l,m}^*$ , and integrating over the solid angle. The coefficients can be written as

$$a_{lm} = \int r(\theta, \phi) Y_{l,m}^*(\theta, \phi) d\Omega \quad (12)$$

Choosing each angle to correspond to the points of a Gaussian quadrature the evaluation of these integrals is straightforward. A set of coefficients, once determined, then serve as a complete mathematical characterization of the aggregate of particles. Many properties of the shape can be computed once the spherical harmonic expansion is known. These include volume, surface area, curvature and the moment of inertia tensor, as before mentioned. These coefficients are unique and can, therefore, be

used directly as a feature vector for describing the shape. In this manner, a spectral decomposition of any (square-integrable) function may be carried out. Examples where similar techniques have been applied include characterization of protein folding [13] in the bioinformatics field and existence of cement aggregates in construction [14] relevant to engineering.

### 3 Simulation results

The simulations are carried out in the  $NVT$  ensemble with a fixed number of particles  $A$ . The volume  $V$  at a fixed baryon density  $\rho$  is simply  $V = A/\rho$ . In the computer simulation we initially place the finite nuclear system under study, initially distributed uniformly inside a cubic box of volume  $V = L^3$ . We fix temperature at  $T = 1$  MeV in order to somewhat simulate quantum motion proper of fermions. Then we allow particles to interact according to the Hamiltonian described in the previous section. Once the thermalized stable clustered configurations are obtained, we statistically sample the system for the averaged structure properties of interest. To minimize finite-size effects we use periodic boundary conditions.

In Fig. 1 we can see a typical clustered configuration arising from our simulations. This particular sample has been obtained at  $T = 1$  MeV,  $\rho = 0.016 \text{ fm}^{-3}$  and a lepton fraction  $Y_e = 0.2$ . A typical representative cluster has  $A^c = 120$  and  $A_n^c = 85$ . In Fig. 2 we can see the moment of inertia tensor components for a representative cluster arising from the configuration shown in Fig. 1 versus the number of spherical harmonics used in the expansion,  $n$ . The cluster shape is somewhat prolate  $I_{33} > I_{11}$ . For expansions using  $n > 20$  there is a rapid convergence. Smaller crossed components for the moment of inertia tensor show departure from ellipsoidal shape. Nucleon mass has been set to  $m = 1$ . In Fig. 3 we plot volume and surface area for a representative cluster arising from the configuration shown in Fig. 1, versus  $n$ . We have chosen a Gaussian quadrature of 100 points. We can associate an average spherical matter radius

**Fig. 1** Typical pasta structures arising in our nuclear simulation at  $T = 1$  MeV,  $\rho = 0.016 \text{ fm}^{-3}$  and  $Y_e = 0.2$

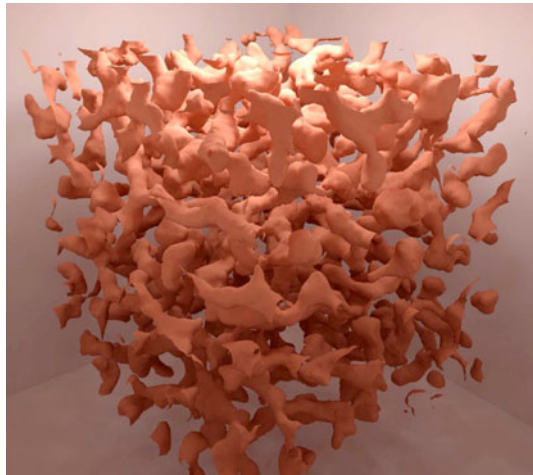


**Fig. 2** Moment of inertia tensor components for a typical cluster in the configuration of Fig. 1. Mass of nucleons is set  $m = 1$

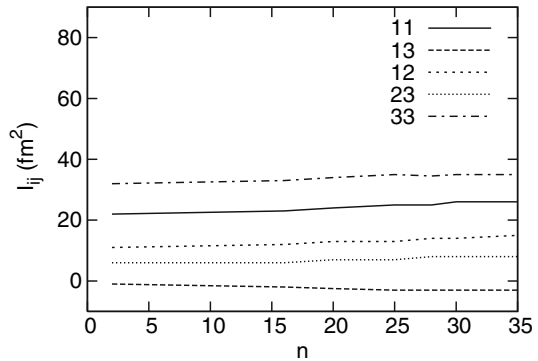
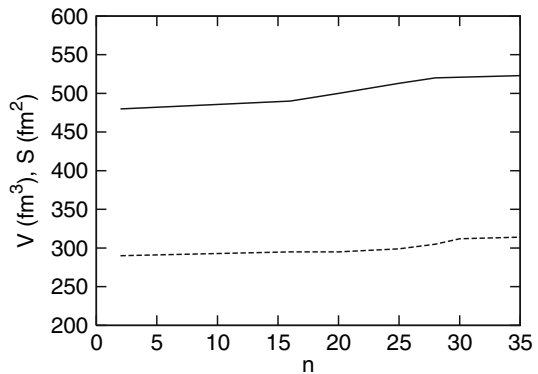


**Fig. 3** Volume and surface area of a typical cluster in the configuration of Fig. 1



of  $r \approx 5$  fm. The liquid drop formula gives an estimate  $R = 1.1[A^c]^{1/3} \approx 5.4$  fm. As clearly seen, rapid stabilization occurs for  $n > 20$ . Further work is necessary to characterize the density and temperature dependence as the cluster shape changes and the relevance to neutrino opacities. It will be published elsewhere. Parametrization in terms of structure functions [2] has allowed some preliminary study of these effects.

To conclude we have presented a method to analyze the shape of clusters arising in low density neutron rich matter present in the crust of neutron stars. The surface of the nuclear cluster is treated as a (single-valued) function of the spherical coordinates,  $(r, \theta, \phi)$ , that can then be expanded in a linear combination of spherical harmonics. The use of spherical designs for the integration provides a robust, fast and elegant approach for the determination of the expansion coefficients and, in turn, the observables available from them can be computed to gain insight into their further thermodynamical dependence.

**Acknowledgments** This work has been partially supported by the Ministry of Education and Science under project DGI-FIS2006-05319. We acknowledge the financial support of the Junta de Castilla y Leon under the “Programa de Financiación de la Actividad investigadora del Grupo de Excelencia GR-234”.

## References

1. D.G. Ravenhall, C.J. Pethick, J.R. Wilson, Phys. Rev. Lett. **50**, 2066 (1983)

2. C.J. Horowitz, M.A. Pérez-García, J. Piekarewicz, Phys. Rev. C. **69**, 045804 (2004)
3. C.J. Horowitz, Phys. Rev. D. **55**, 4577 (1997)
4. B.D. Serot, J.D. Walecka, Adv. Nucl. Phys. **16**, 1 (1986)
5. M. Metropolis et al., J. Chem. Phys. **21**, 1087 (1953)
6. M.P. Allen, D.J. Tildesley, *Computer Simulation of Liquids* (Oxford University Press, Oxford, 1989)
7. J. Vigo-Aguiar, T.E. Simos, A. Tocino, Int. J. Mod. Phys. C. **12**, 225 (2000)
8. N. Itagaki et al., Nucl. Phys. A. **738**, 17–23 (2004)
9. M.A. Pérez-García, K. Tsushima, A. Valcarce, Int. J. Mod. Phys. E (in press)
10. M.A. Pérez-García, K. Tsushima, A. Valcarce, Phys. Lett. B. **660**, 600 (2008)
11. M.M. Sharma, S. Mythili, A.R. Farhan, Phys. Rev. C. **59**, 1379 (1999)
12. G. Arfken, *Mathematical Methods for Physicists* (Academic Press, Boston, 1985)
13. R.J. Morris et al., Bioinformatics **21**(10), 2347–2355 (2005)
14. C. Garboczi, Cem. Concr. Res. **32**(10), 1621–1638 (2002)